# Spectroscopy of Amorphous and Crystalline Titania−Silica Materials

**Allison S. Soult,[‡] Donald F. Carter,[‡] Henry D. Schreiber,[†] Lambertus J. van de Burgt,[‡] and A. E. Stiegman*[,‡]**

*Department of Chemistry and the Materials Research and Technology Center (MARTECH), Florida State University, Tallahassee, Florida 32306, and Department of Chemistry, Virginia Military Institute, Lexington, Virginia 24450*

*Received: March 27, 2002*

Both amorphous and crystalline silica doped with Ti(IV) ions have properties ranging from selective chemical catalysis to useful thermal and optical characteristics. These properties are related to the distribution of titanium sites in the silica lattice. It has been proposed that the Ti(IV) isomorphically substitutes for Si in the lattice in an essentially tetrahedral geometry. In this study we compare the electronic and vibrational spectroscopic characteristics of a series of both dense and porous amorphous titania−silica materials with crystalline titania−silicalite (TS-1). All of the spectroscopic properties are referenced to titania−cristobalite, which contains titanium in a rigorous crystallographic environment that deviates only slightly from tetrahedral. It is found that the amorphous materials have spectroscopic properties that are extremely close to Ti-cristobalite while TS-1 deviates significantly.

## Introduction

Both amorphous and crystalline binary titania−silica materials are of interest because of their useful physical and chemical properties. For example, dense amorphous titania−silica glass has a significantly higher refractive index than fused quartz, depending on the titanium concentration, and an anomalously low coefficient of thermal expansion.[1,2] These properties have led to their commercial exploitation as thin film and as bulk optical materials. On the other hand, porous titania silicalite (TS-1) zeolites and xerogels have fostered considerable study due to their effectiveness as a selective oxidation catalyst, the former of which has found application commercially in the oxidation of phenol to hydroquinone.[3−5]

In all of these materials, the useful properties originate from the coordination environment and electronic structure of the titanium sites distributed in the silica matrix. For TS-1, catalysis occurs through discrete Ti(IV) centers in the zeolite matrix while for amorphous titania−silica glass, the titanium exists in discrete, isolated sites at low concentration with large clusters or oligomers appearing at higher concentration. For all of these materials and, in particular, TS-1, it has been suggested that in the discrete limit titanium isomorphically substitutes for silicon in tetrahedral positions in the matrix.[3,4] While a number of experimental techniques have been applied to confirm this suggested structure, few have compellingly eliminated other, lower symmetry, four-coordinate structures. One problem with unambiguous structural characterization lies in the fact that titanium does not favor tetrahedral coordination in an oxide matrix. This both increases the need for unambiguous experimental evidence since such geometry is not expected and increases the difficulty in obtaining it since there are few oxides containing tetrahedral titanium with which comparisons can be made.

Recently, we have reported luminescence originating from discrete titanium sites located in the silicalite lattice of TS-1.[6] This observation has facilitated a more precise assignment of the zero-point energy of the first excited state, which proved to be significantly lower than previously thought. It also facilitated the assignment of the 960 $cm^{-1}$ band in the vibrational spectrum of these materials. In this study we report the electronic and vibrational spectra of titanium sites in amorphous and crystalline titania−silica materials. We compare these spectroscopic properties to titania−cristobalite in which titanium sits in a nearly tetrahedral silica lattice. We believe that this comparison provides insights into the structure of titanium in these materials and, for specific materials, provides good evidence for the proposed tetrahedral structure.

## Experimental

**Synthesis.** Titania−silica sol−gel glasses up to 12 mol % [100 × moles Ti/(moles Ti + moles Si)] were made by the co-condensation of tetramethyl orthosilicate (TMOS) and titanium tetraisopropoxide with 2-propanol as a cosolvent. In a typical preparation for a 1 mol % sample, 20.4 mL of TMOS (Gelest, 99+%) was added to a flask containing 39.6 mL of 2-propanol (Aldrich, HPLC grade) with constant stirring. A 0.417 mL aliquot of titanium tetraisopropoxide (Aldrich, 99.999%) was then added to the flask and the solution was allowed to mix thoroughly (≈1−2 min). A solution containing 33.2 mL of 2-propanol, 6.36 mL of Nanopure water (18 mΩ Barnstead E-Pure System), and 1.21 mL of hydrochloric acid (Fisher, Optima Grade) was then added at a rate of approximately 1 drop per second. The drip rate could be slightly increased for lower concentration samples and, correspondingly, decreased for higher concentration samples. The clear solution was then dispensed into 4 mL polystyrene cuvettes, capped, and allowed to gel. After gelation, the caps were punctured to allow evaporation of the solvent. The final samples were hard transparent monoliths with the approximate dimensions of 0.5 × 0.5 × 1.2 cm. The aged and dried monoliths were carefully

* Corresponding author.
[†] Virginia Military Institute.
[‡] Florida State University.

10.1021/jp020812c CCC: $22.00 
Published on Web 08/17/2002

placed in a ceramic crucible and heated at a rate of 5 °C per hour to 100 °C where they were held for 72 h and then heated to 500 °C where they were then held for 36 h. After calcination the samples were allowed to cool slowly (5 °C/h) until they reached room temperature.

Titanium-cristobalite was synthesized from titania−silica xerogels following a reported procedure.[7] Titania−silica xerogels containing 0, 0.05, 0.5, 2, 5, and 7 mol % titanium in platinum crucibles were placed in an 800 °C furnace under air where they were then taken to a temperature of 1500 °C over a period of 7 days. The samples were then quenched to ambient temperature. X-ray analysis showed them to be authentic cristobalite. The materials exhibited a linear increase in unit cell volume as a function of titanium concentration indicative of incorporation into the crystal lattice and consistent with previous reports.

**Electronic Spectroscopy.** Emission spectroscopy was carried out on a Spex Fluorolog II equipped with 0.22 m double monochromators (Spex 1680) and a 450 W Hg/Xe lamp. Right angle (90°) collection was used to collect both emission and emission excitation spectra. Cutoff filters were used to suppress second-order excitation lines. Reproducible emission spectra were attained after calcination of the samples at 500 °C under a flow of oxygen (UHP grade). Since it was imperative that they not experience ambient laboratory conditions again prior to data collection, they were taken from a tube furnace directly into an antechamber under a dry $N_2$ purge where they were mounted in an APD model DE-202 cryostat, shrouded, and evacuated. The samples were carefully aligned to maximize intensity in the detector prior to collection of spectra to ensure the best reproducibility of emission intensities. All reported spectra were corrected for the lamp profile and the detector response. Spectra reported in wavenumber units were corrected in the standard way for the band-pass variability of spectra collected at fixed wavelength resolution. Because of the spectral congestion on the blue edge of the titanium emission, the full width at half-height (fwhh) for the titanium emission band was estimated by doubling the value of the half width at half-height measured from the low energy side of the emission band.

**Time-Resolved Emission.** Fluorescence was induced using 355 nm excitation pulses produced from a frequency tripled DCR-2a 10 Hz pulsed Nd:YAG laser system (Spectra-Physics) with a 9 ns pulse time width and an 8 mm beam diameter. A 0.25 m (f/3.6) Ebert monochromator model 82−410 (Jarrell-Ash.) was the dispersive element prior to the detector, which is a Hamamatsu R928 extended red high sensitivity side-on type photomultiplier tube (PMT) with all dynodes employed. The signal from the PMT was coupled to the oscilloscope with 5.0 kOhm load resistor. A LeCroy model 9410 dual-channel 150 MHz digital oscilloscope was used in the collection and handling of data.

Data analysis was carried out on the emission decays, collected at 274 K over a range of monitoring wavelengths from 450 to 650 nm. Following previous protocols and analysis, fits of the overall emission decay curve were carried out using a biexponential ($I/I_0 = ae^{-t/\tau} + be^{-t/\tau'}$) decay function where $I$ is the intensity, $t$ is time, and $\tau$ is the lifetime. Decays were fit starting from 5% after the initial spike to avoid convolution with the exciting light. The relative contribution of the two lifetimes (obtained from the preexponential factors of the biexponential fit) to the total emission decay varied systematically as a function of wavelength. The short-lived component ($\tau_1$) becomes the dominant contribution as the wavelength increases until, at $\lambda \geq 550$ nm, it accounts for ≥87% of the total decay. Based on this observed trend we assign the short-lived component to the titanium emission and the longer-lived component to the intrinsic silicalite background emission.

**Raman Spectroscopy.** Raman spectra of homogeneous titania−silica xerogels were collected at 90° from the incident radiation, which passed through the center of the transparent monolithic sample, sealed in a 5 × 5 mm quartz fluorescence cell. All samples were baked out at 500 °C under an oxygen flow for 12 h in the sample holder and then closed off under vacuum just prior to measurement. Incident radiation was from the 488.0 nm (∼1 W) line of a continuous wave argon ion laser (Coherent Innova-90). Inelastic scattering was collected through a 0.85 m f/7.8 double grating spectrometer, modified Czerny-Turner operating in additive dispersion, (Spex 1403) having 2400 groove/mm gratings, 102 × 102 mm, cosecant drive to allow linear frequency scanning. The laser line was filtered using a Spex 1460 Lasermate grating monochromator before entering the macro-sampling chamber, Spex 1459 UVISIR Illuminator. Samples are mounted in an XYZ, micrometer-controlled, translation stage. Detection was with a Burle C31034 11 stage GaAs photomultiplier (dark noise of 30−100 counts/second) contained in a thermoelectrically cooled housing (Products for Research) and operated in single photon counting mode using an external preamplifier-discriminator having <40 ns pulse-pair resolution and a digital photon counter, Spex DPC-2. Polarization anisotropy was measured by inserting a linear polarizer in the scattered light path oriented either parallel to or perpendicular to the exciting laser line. The resultant parallel polarized and perpendicular polarized spectra directly yield the polarization anisotropy. Polarization bias in the spectral intensity due to the gratings was avoided by use of a polarization pseudo-scrambler in the collection optical path.

Raman spectra of cristobalite and titanium-cristobalite were obtained using a micro Raman spectrograph, the JY Horiba LabRam HR800, excited by a Coherent I-308 argon ion laser emitting 200 mW of power at 488 nm. The spectrograph uses a holographic notch filter to couple the laser beam into the microscope (Olympus BX30) by total reflection. The beam is focused on the sample through a microscope objective (20× for the undoped cristobalite and 50× IR (Leica) for the 0.5% Ti-cristobalite). The laser power is 10 mW at the sample. Scattered radiation is collected by the objective and the laser radiation is filtered out by the notch filter with Raman scattering coupled into the spectrograph through a confocal hole. A 76 mm square 600 line/mm grating disperses the Raman scatter onto a 1024 × 256 element open electrode CCD detector (Wright) having 26 $\mu$m square pixels thermoelectrically cooled to −70 °C. The detector has a quantum efficiency of 35−42% around 500 nm. Spectral resolution, determined by the confocal hole size, is 7 $cm^{-1}$ for the undoped cristobalite (250 $\mu$m hole) and 2 $cm^{-1}$ for the 0.5% Ti-cristobalite (50 $\mu$m hole). Although the spectral resolution for the undoped cristobalite is 5 times that of the 0.5% Ti-cristobalite, the 1080 $cm^{-1}$ peak width changes from 16 $cm^{-1}$ to 12 $cm^{-1}$. Thus, the instrument resolution for the Ti-doped spectrum is narrower than the spectral width of the sample. Fifteen pixels in each CCD column were binned and 8 spectra were collected for 30 s exposures for the undoped sample and 4 spectra were exposed for 300 s for the 0.5% Ti-cristobalite. The doped sample was exposed for a longer time period to offset the lower light throughput due to the smaller confocal hole setting.

**ICP-Mass Spectrometry.** To assess the purity of the materials and determine the amounts of Sn and Ge in the samples, analysis was carried out using inductively coupled plasma mass

spectrometry (ICP-MS). The instrumentation was a Finnigan MAT Element ICP-MS with a Glass Expansion MicroMist nebulizer. The nebulizer gas flow (Ar) was 1.06 L/min. The cooling gas flow was 13 L/min and the ICP power was 1300 W. ICP-MS was used to determine the purity of the samples by analyzing the concentrations of metal species in a variety of samples. One hundred milligrams of each sample was dissolved in 1 mL of quartz distilled water along with 5 mL of a 1:1 HF:$HNO_3$ solution. They were then dried and redissolved in 1 mL of 7 N $HNO_3$. Approximately 0.5 mL of this solution was diluted to a 1% solution with 1% $HNO_3$. These were the stock solutions from which further dilutions were made for analysis. Three samples were made from each stock solution, all containing an In reference which allowed us to account for instrumental drift. The first sample contained only the In, while the second and third sample contained one and two aliquots, respectively, of a solution containing known amounts of Sn and Ge. These standard additions gave us the ability to determine the concentration of Sn and Ge with much higher accuracy than using a reference solution.

**Infrared Spectroscopy.** FT-IR spectra were collected as diffuse reflectance spectra on a Nicolet Nexus 470 FT-IR with the Harrick Praying Mantis Diffuse Reflectance Attachment. The samples were heated to 500 °C prior to mixing with KBr (10 wt % of xerogel sample). Once in the reaction chamber, the sample was then heated to 300 °C for 30 min and then cooled and the spectra collected.

## Results and Discussion

**Amorphous Titania−Silica Xerogels.** The photoemission spectra of Si and Ti/Si xerogels, as a function of titanium concentration are shown in Figure 1. The pure silica control shows an asymmetric emission band centered around 416 nm with a sharp peak at 391 nm and a resolved shoulder at 462 nm. Addition of titanium results in the emergence of a broad band at 475 nm that becomes larger, relative to the high energy 416 nm band, as a function of titanium concentration. At the highest concentration of titanium investigated (6 mol %), the high-energy band appears only as a shoulder on the blue edge of the broad emission at $\lambda_{max} = 475$ nm. This pattern of emission bands and the observed concentration dependence parallels that observed in TS-1 and, consistent with our previous analysis of that system, we assign the 475 nm band to emission from the titanium sites and the high-energy 416 nm band as resulting from an emission intrinsic to the silica matrix.[6]

The emission, emission excitation, and electronic absorption spectrum for a 0.5 mol % titanium xerogel are shown in Figure 2. As can be seen from the absorption spectrum, there are no obvious electronic absorptions, just a gradual increase in intensity until 32 000 $cm^{-1}$ when the absorption starts to increase dramatically. Since the emission is centered at 20 700 $cm^{-1}$ this high-energy absorption cannot represent direct excitation into the emitting state as that would indicate a nonphysical Stokes shift. For this reason there must be weak transitions to lower energy in the region from approximately 24000 to 27000 $cm^{-1}$; one of which is a direct excitation into the emitting state. Some evidence for this can be seen in the emission excitation spectrum, which does show resolvable bands in this region. This suggests a strongly nonallowed excited state with the only intense transitions coupled to it lying at significantly higher energy. Consistent with this description, the excited state is relatively long-lived with a 0.58 $\mu$s lifetime at room temperature. These spectroscopic properties are broadly similar to those observed for TS-1.[6]

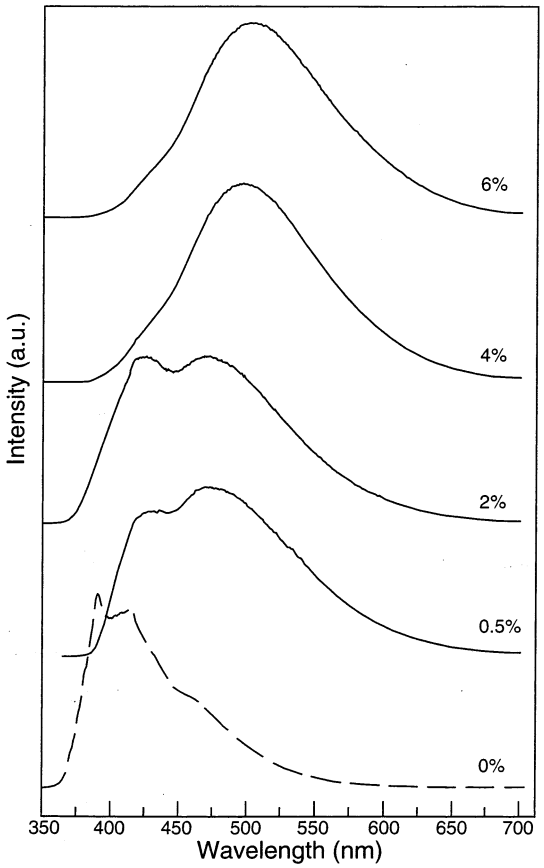


**Figure 1.** Emission spectra, collected at 10 K (280 nm excitation) of titania−silica xerogels as a function of the mole % of titanium present.

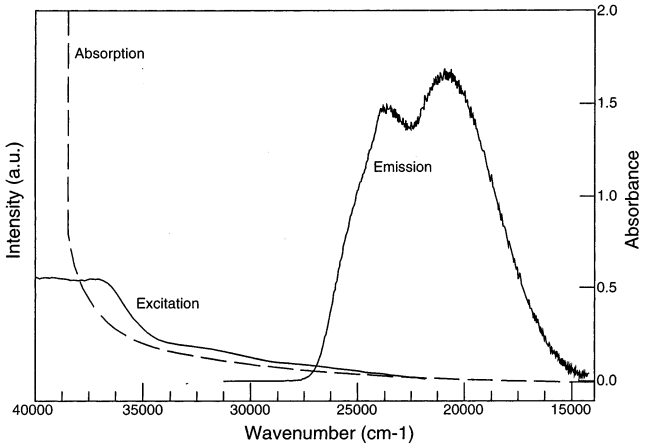


**Figure 2.** Emission, emission-excitation, and absorption spectra for a 0.5 mol % titania−silica xerogel. Emission and emission excitation spectra were collected at 8 K with 350 nm excitation and 600 nm monitoring, respectively. Absorption spectrum collected at RT.

When titanium is distributed in an amorphous silica network it would be anticipated that discrete, isolated metal sites exist only at lower concentrations while at higher concentrations oligomeric or clustered structures containing Ti−O−Ti bonds would be expected. For titania−silica xerogels the emission peak is assignable as emanating from discrete isolated sites since it is observed at very low concentrations (0.005 mol %) of titanium. The intensity of the band increases with titanium concentration; however, even at concentrations approaching 6 mol % there are no discontinuous changes in the spectrum and, more importantly, no new emission features emerge. This suggests that the emission is coming only from the isolated

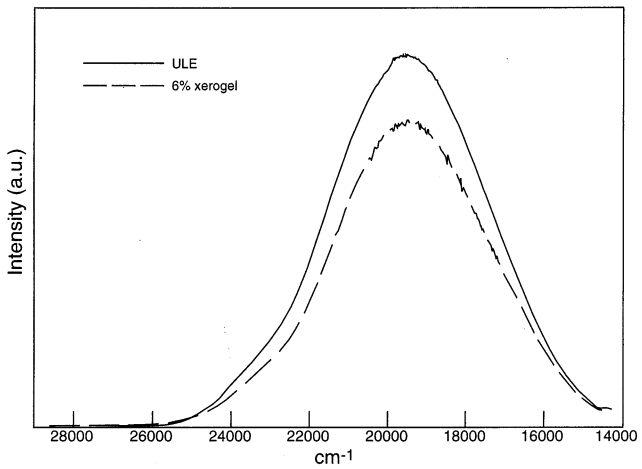


**Figure 3.** Emission spectra of 6 mol % titania−silica xerogel (—) and ULE glass (− − −) collected at 10 K at 280 nm excitation.

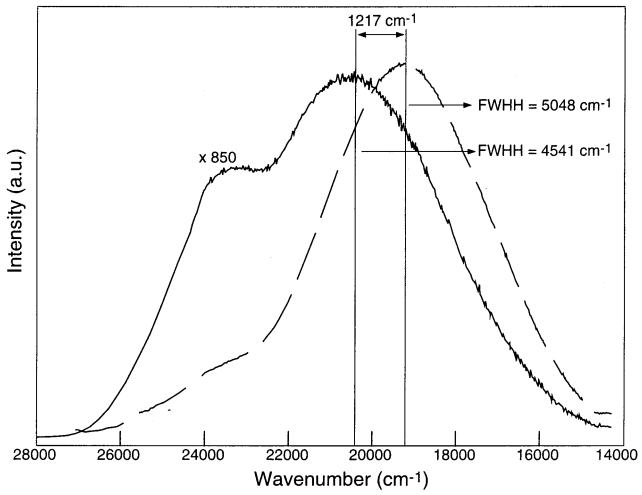


**Figure 4.** Emission spectra of 2 mol % titania−silica xerogel (− − −) and TS-1 (—) collected at 77 K at 280 nm excitation.

species and that any oligomerized or clustered titania species tend to be nonemissive.

**Comparison to Dense Titania−Silica Glass and TS-1.** An emission spectrum of commercially produced titania−silica ULE glass containing ∼7% titanium and a porous xerogel of comparable concentration are shown in Figure 3. The $\lambda_{max}$ for emission for the two materials is identical as is the band shape, which indicates that the emitting site is essentially unaltered upon densification of the matrix. Consistent with this, the lifetime of the excited state in ULE is 0.86 $\mu$s, which is close to the value obtained for the xerogels. In addition, the dense, commercially produced material, also exhibits the same high-energy background emission band that is observed in titania xerogels and in TS-1. The useful property of ULE glass is its small coefficient of thermal expansion (CTE), which approaches zero between 0 and 100 °C and is zero (±30 ppb) between 5 and 35 °C.[2] A significant question is how, on a molecular level, the titanium influences the coefficient of thermal expansion. In crystalline materials a low or negative CTE is often traceable to defined contractions in specific bonds in the crystal.[8] If the low CTE is due to changes in the Ti−O bond lengths, which act to compensate for the expansion of the silica as the temperature increases, then photoemission is likely to be sensitive to these changes. Emission spectra of ULE glass collected at a range of temperatures from 8 to 573 K showed only the expected decrease in intensity with no variations in the position or shape of the band observed. This may suggest that the species responsible for the low CTE is nonemissive; possibly an oligomeric species or cluster.

Figure 4 shows the emission from 2.0 mol % titania−silica xerogels and titania silicalite (TS-1) collected at 77 K. The high-energy background emission is observed in the same position in both spectra though the relative contribution of this band to the total emission differs between them at this excitation wavelength. The titanium emission in TS-1 occurs 1217 cm$^{-1}$ higher in energy than it does in the amorphous materials. The lifetimes of the emitting sites also differ with the amorphous materials being shorter lived by 2 orders of magnitude than TS-1 (0.58 $\mu$s vs 81 $\mu$s at RT). Notwithstanding the energy and lifetime differences, the band shape and the full-width at half-height are, in fact, quite similar (4541 and 5048 cm$^{-1}$ for titania−silica xerogel and TS-1, respectively). This tends to suggest a basic similarity in the chromophores with the observed energy changes arising from structural perturbations that increase the energy of the charge transfer. Additional support for this conjecture comes from vibrational spectroscopy. For TS-1 there

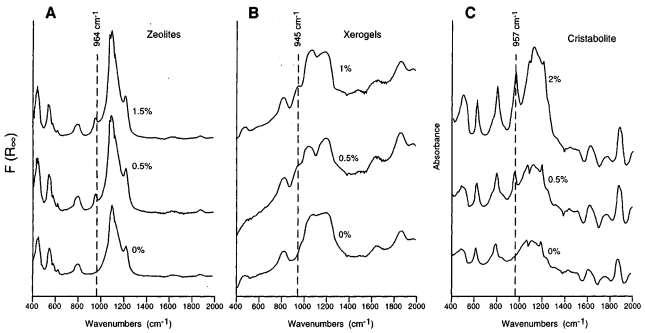


**Figure 5.** Infrared spectra, collected as diffuse reflectance spectra and plotted in Kubelka−Munk units, for (a) titania-silicalite, (b) titania xerogels, and (c) titania-cristobalite.

is a well-studied Ti−O−Si stretching mode at 960 cm$^{-1}$ that is strongly coupled to the emitting state.[4,9] As shown in Figure 5, an analogous vibration is present in the infrared spectra of titania−silica xerogels where it is observed as a shoulder at ≈945 cm$^{-1}$. In addition, both TS-1 and the amorphous titania−silica xerogels have a high-frequency mode associated with titanium in the region of 1100 cm$^{-1}$. This band is not observable in the infrared due to interference by the intense silica bands but can be seen by Raman spectroscopy. Recently, Ricchiardi et al. has assigned these bands using density functional calculations of discrete tetrahedral $Ti(OSi(OH)_3)_4$ clusters.[10] This study assigns the high-frequency band to a symmetric mode in the $TiO_4$ tetrahedron arising from the in-phase antisymmetric stretch of the Ti−O−Si bonds. The low energy 960 cm$^{-1}$ band was assigned to an antisymmetric Ti−O−Si stretch that was coupled to the Si−OH stretch of free silanol groups. A detailed Raman study of completely dense titania−silica glass has been reported previously by Knight, Pantano and White.[11] These dense materials showed titanium-dependent bands at 935 and 1105 cm$^{-1}$. The 1105 cm$^{-1}$ band was shown to be strongly polarized and, hence, totally symmetric while the 935 cm$^{-1}$ was clearly antisymmetric. The porous xerogels reveal similar properties (Figure 6) with a symmetric stretch at 947 cm$^{-1}$and an antisymmetric stretch at 1102 cm$^{-1}$. The similarity in the observed vibrational spectra between all of these materials suggests a similarity in the structure of the titanium site. Furthermore, the observed polarizations are consistent with the cluster-based assignments of Ricchiardi. However, the inclusion of coupling to silanol to explain the energy of the 960 cm$^{-1}$ band is clearly incorrect since these bands are present in totally

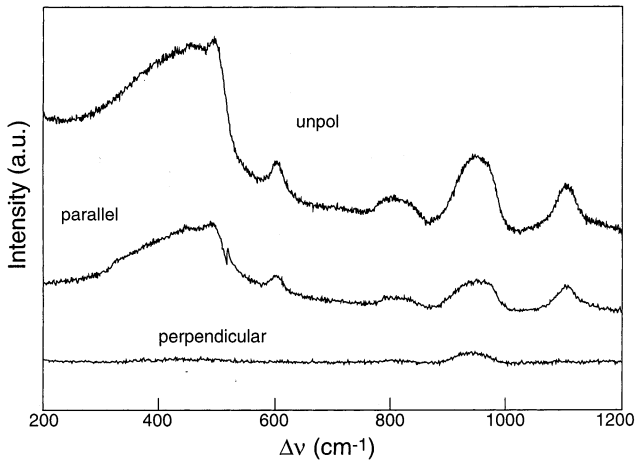


**Figure 6.** Unpolarized, parallel, and antiparallel polarized Raman spectra (488 nm excitation) of 3 mol % titania−silica xerogels.

dense, and hence silanol-free, titania−silica glasses. The need to include such coupling to achieve the correct energy is probably an artifact of the cluster approximation.

**Spectroscopic Properties of Titanium in α-Cristobalite Matrix.** Microcrystalline titanium-substituted α-cristobalite was made by heating titania silica xerogels to 1500 °C followed by quenching to ambient temperature. These materials are of interest as spectroscopic models because the titanium will be forced into a tetrahedral silicon oxide ligand field due to the crystallographic constraints of the α-cristobalite lattice. For the α phase of cristobalite, which is produced here, the geometry around the T-site will not be rigorously tetrahedral but tetragonally distorted with two long and two short Si−O bonds (1.606(2) and 1.588(2) Å) and O−Si−O angles that deviate from ideal tetrahedral.[12] We note, however, that some caution must be exercised in assuming isomorphic substitution by titanium in α-cristobalite since cristobalite has interstitial vacancies that could, in principle, accommodate the titanium in a six-coordinate environment. A series of titania-cristobalite samples, with varying Ti concentration, were made and investigated by Evans as part of a study of low CTE titania−silica glasses. These studies showed very good agreement between the observed changes in unit cell volume with titanium substitution and the volumes predicted from random isomorphic substitution of Ti for Si in the lattice.[13] In addition, prior studies of Ti incorporation into cristobalite and tridymite have suggested that the structural voids in cristobalite cannot easily accommodate large cations (as opposed to those of tridymite) and, as a result, small amounts of Ti are incorporated through substitution of the Si.[14,15] Finally, as we will show, the general spectroscopic properties (vibrational and electronic) of Ti-cristobalite compare quite closely to amorphous Ti−silica glasses and to TS-1; both of which have four-coordinate environments. As a result, we can, with some confidence, assume the titanium site to be essentially tetrahedral in this material thereby making it a good model.

Figure 7 shows the emission spectrum of 0.5% Ti-cristobalite collected at 12 K. As in the other titania−silica materials, the spectrum is composed of two bands, the higher energy background emission is present at approximately the same position (23000 $cm^{-1}$) as it is in TS-1 and the amorphous materials. Emission from titanium sites appears, as it does in those materials, to lower energy. At this titanium concentration evidence of a vibrational progression appears with two resolved peaks at 21709 and 19867 $cm^{-1}$ and a shoulder at ∼18260 $cm^{-1}$. As was observed with TS-1, higher concentrations of Ti resulted in an increase in the intensity of the low energy emission but

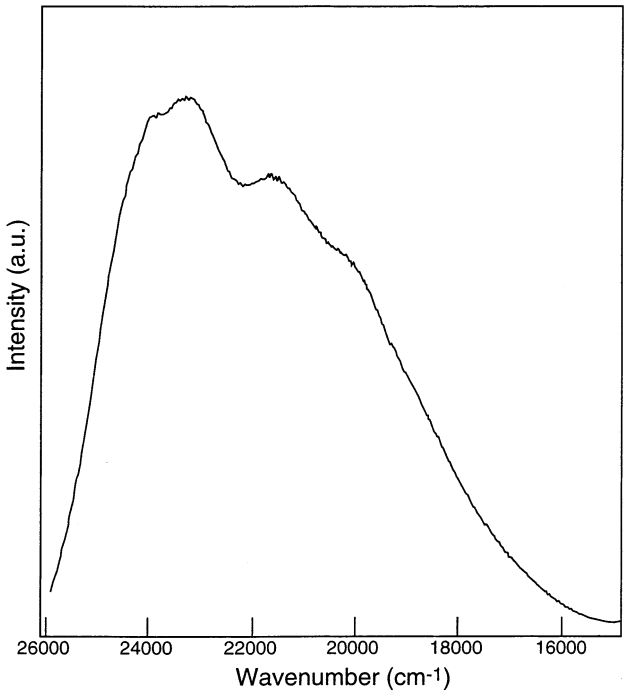


**Figure 7.** Emission spectrum of titania-cristobalite (0.5 mol %) collected at 12 K at 280 nm excitation.

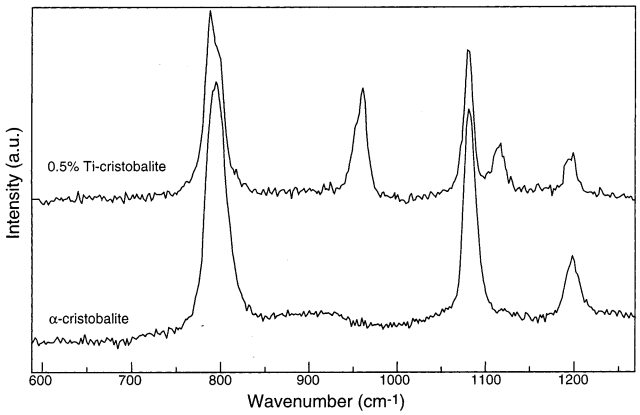


**Figure 8.** Raman spectra of cristobalite (bottom) and 0.5 mol % titania-cristobalite at 785 nm excitation.

resolution of the vibrational modes was lost above 0.5 mol %. For 0.5% Ti-cristobalite, the large amount of spectral overlap and the weakness of the emission make the analysis of the vibrational structure problematic. However, the active mode appears to be greater than 1000 $cm^{-1}$. This differs from TS-1, which clearly showed a progression in the low frequency (960 $cm^{-1}$) mode. Importantly, the vibrational spectra of the titania-cristobalite compares closely to all of the other Ti−silica materials. The infrared spectrum (Figure 5) shows a titanium-dependent band at 957 $cm^{-1}$, assignable, by analogy, to the antisymmetric Ti−O−Si stretch. The Raman spectrum (Figure 8) of 0.5% Ti-cristobalite also shows this band and a high-frequency band at 1117 $cm^{-1}$. It appears that as the titanium site approaches a true tetrahedral geometry the vibronically active mode is the high-frequency symmetric mode and not the 960 $cm^{-1}$ antisymmetric mode.

As can be seen in Figure 9, the emission from the titania-cristobalite is quite close in energy and in band shape to the amorphous materials. This indicates that even when the coordination environment is not crystallographically constrained, the distribution of geometries around the metal appear to average

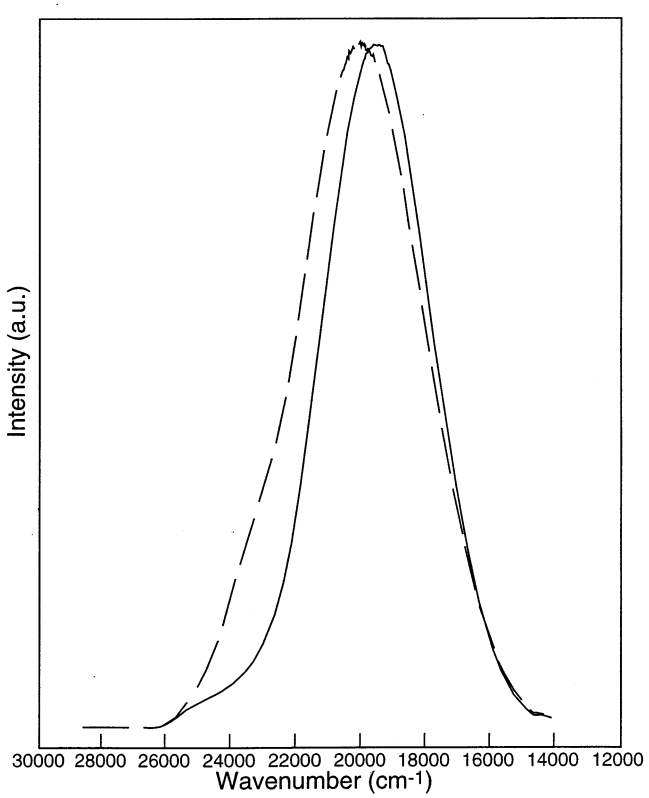


**Figure 9.** Emission spectra of 0.5 mol % titania-cristobalite (—) and 4 mol % titania xerogel (− − −) collected at 12 K at 280 nm excitation.

to a value close to tetrahedral. For TS-1, the emission energy is significantly higher than in either the amorphous or cristobalite matrix. Likewise, the Ti−O−Si stretches (both symmetric and antisymmetric) also occur at higher energy. This suggests structural and, as a result, electronic characteristics that differ quantitatively from those observed in a true (or close to true) tetrahedral environment. Notwithstanding this, the qualitative similarities in the spectra tend to suggest a gross similarity in all of these titanium sites. This is not inconsistent with proposed binding of titanium in the silicalite lattice in which the site experiences a high degree of distortion due to the overriding crystallographic constraints of the lattice (just as cristobalite enforces a tetrahedral geometry). This distortion, which reduces the site symmetry below Td, could easily account for the increase in energy and decrease in extinction coefficient in the first electronic transition as orbital mixing changes. Furthermore, these structural/electronic differences could also account, at least in part, for the greater catalytic reactivity of TS-1 over titania supported on amorphous silica.

**Assignment of the High-Energy "Background" Emission.** The asymmetric emission band at ∼420 nm is observed in all samples regardless of titanium content and preparation, including the completely dense, commercially produced ULE glass (Figure 10). In titanium-free control samples, measured at cryogenic temperatures, this emission envelope can be resolved into several distinct bands; the number and sharpness of which depend somewhat on the matrix. Regardless of the matrix, however, there are two principal bands that always appear; one is the more intense transition that defines the emission maximum at ∼420 nm and the other is a resolved shoulder at ∼462 nm. The relative intensities of these two bands are excitation independent, suggesting that they are assignable to the same emitting species. In the pure silica xerogel (Figure 10) an additional very sharp peak is resolved at 391 nm, which is not evident in any of the other materials. This peak appears to arise

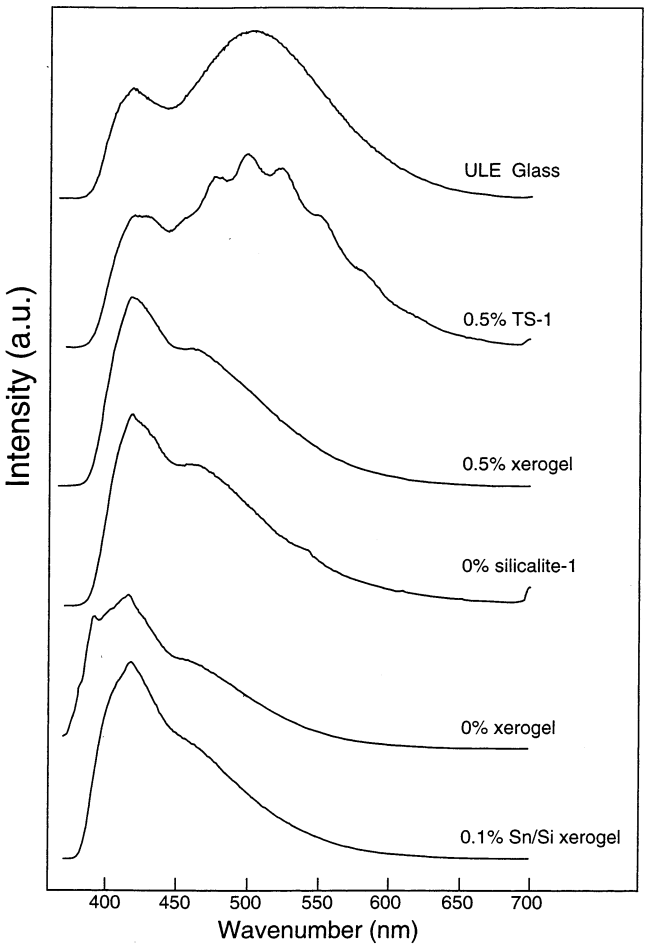


**Figure 10.** Emission spectra for a silica and titania− and tin−silica matrixes collected at 77 K and 280 nm excitation.

from a different emitting site as it varies with excitation intensity relative to the 420 and 462 nm peaks. In addition, in pure silica xerogels a broad featureless emission is observable in the near UV at 355 nm with high-energy excitation (290 nm). This clearly indicates that there are multiple emission peaks observable in the matrix of silica-based materials produced through sol−gel and related processes that are assignable to intrinsic defects in the matrix or to impurities introduced during synthesis.

Notwithstanding the number of intrinsic emitting sites, the asymmetric emission band at ∼420 nm appears to be ubiquitous and often interferes with luminescence that may be of interest. It has also been observed in the luminescence from vanadium-substituted silica $\beta$-zeolites where it was assigned as emission from OH groups in the matrix (its presence in completely dense ULE glass effectively precludes this assignment).[16] The fact that this emission is present in such a wide range of materials, all of which are synthesized from a common set of starting materials, strongly suggests that it originates from impurities intrinsic to the reagents or is otherwise introduced during synthesis. In our previous study on TS-1, which were prepared using high purity reagents, the type and amount of trace contaminants was determined using inductively coupled plasma mass spectroscopy (ICP-MS). This study found that the most common impurities which appeared in quantities greater that 10 ppb were alkali metals, the transition metals Zr, Cr, F, Cu, and Zn, and the main group elements Sn and Te. Other main group elements such as Ge, Ga, Al, In, and Pb were present but in quantities less than 1 ppb. By comparison of the emission spectra of silica xerogels in which these elements were intentionally incorporated, it was determined that the 420 nm

**TABLE 1: Concentration of Sn and Ge in Various Ti/Si Samples and Common Reagents**

| sample | Sn (ppb) | Ge (ppb) |
|---|---|---|
| 0.5% Ti/Si silicalite | 2222.10 | 88.66 |
| 0.5% Ti/Si silicalite (high purity)[a] | 357.15 | 58.71 |
| 0.5% Ti/Si xerogel[b] | 4891.16 | 8.56 |
| 0.5% Ti/Si xerogel[b] | 6930.64 | 103.28 |
| 0.5% Ti/Si xerogel[b] | 907.15 | 4401.25 |
| ULE | 684.2 | n/a |
| tetraethyl orthosilicate[c] | 25.32 | n/a |
| tetrapropylammonium hydroxide[d] | 30.81 | n/a |
| titanium tetraisoproproxide[e] | 48.86 | 327.74 |

[a] Scrupulously controlled synthetic conditions and high purity reagents. [b] Synthesized at different times under different conditions. [c] Aldrich, 99.999%. [d] Alfa Aesar, 40 wt % soln. [e] Aldrich, 99.999%.

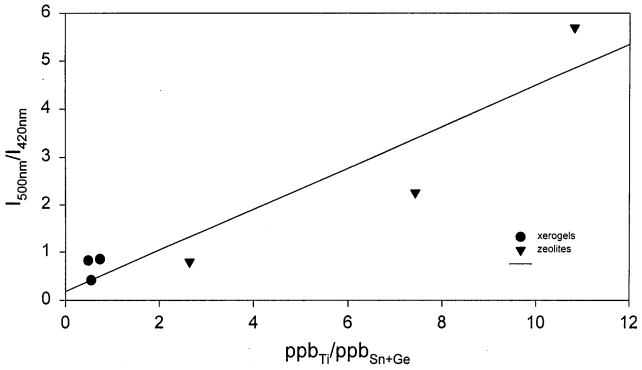


**Figure 11.** Plot of the ratio of the intensity ratio of titanium emission at 500 nm to background emission at 420 nm versus the ratio of titanium to tin + germanium for a series of titania−silica materials.

emission results primarily from the presence of Sn impurities in the matrix. The static and dynamic luminescence properties of isolated Sn sites in silica have been investigated in some depth and the reported emission bands compare closely both in position and in band shape to the intrinsic emission.[17,18] Furthermore, these reports also indicate that germanium has luminescence that is quite close in energy to that of tin and may be indistinguishable if both components are present. By deliberately introducing Sn into silica xerogels, we observed an apparent dramatic increase in the intensity of the 420 nm band when compared to control samples with no general change in its position or shape (Figure 10). Moreover, at cryogenic temperatures it reproduces not only the maximum at 419 nm but also the resolved shoulder at 466 nm. While the specific characteristics of the spectrum strongly suggest that the luminescent impurity is tin (with a possible contribution from germanium) the difficulty in making absolute comparisons in the emission intensity from solid samples still leaves some question. To fully establish that tin is the principal emitting impurity, a variety of titania xerogels and TS-1 samples, made with differing reagent sources and amounts of added titanium, were analyzed to determine their tin, germanium, and titanium concentration. The results of this analysis are shown in Table 1. Using the titanium emission as an internal reference, the ratio of the emission intensities of the impurity (determined at 420 nm) and the titanium emission (determined on the red edge at 500 nm) were plotted against the titanium divided by the amount of tin and germanium [Ti/(Sn + Ge)] actually present in the samples. The plot (Figure 11) reveals a good correlation, which supports the assignment of this particular background emission as arising from Sn and Ge.

Given the importance of purity in these materials, particularly for catalysts such as TS-1, it is instructive to identify sources of Sn and Ge contamination. Since all of the materials are made from the same starting materials, in particular, silicon and titanium alkoxides and, in the case of TS-1, tetrapropylammonium hydroxide we determined the tin and germanium content of commercially obtainable high purity reagents (Table 1). Assuming that all the Sn and Ge in the reagents incorporates into the lattice, a 0.5 mol % sample of TS-1, should give a material with ∼365 ppb combined Sn and Ge. These values are quite close to the actual amount determined for carefully prepared samples of TS-1 (Table 1). For a 0.5 mol % titania xerogel, we would predict 64 ppb Sn. As indicated in Table 1, a number of the xerogels have far higher concentrations of these impurities than can be accounted for by these reagents suggesting that other sources are operative such as glassware, metal needles, and parts. The most likely source, however, are reagent grade acids that are often used to catalyze the process. It is important to note, however, that while Sn and Ge are ubiquitous contaminants in materials derived from these reagents, the amount of these contaminants is still quite small and seems unlikely to affect properties such as catalytic activity.

## Conclusions

It is clear from this study that titania−silica materials, regardless of the form of the matrix, have a number of spectroscopic similarities, both in their electronic and vibrational spectra, which suggest a commonality in the coordination environment of the titanium. Comparison of the spectra of various forms of titania−silica (porous and dense amorphous glasses and crystalline TS-1) to titania-cristobalite, where the titanium is forced into an essentially tetrahedral environment, indicates that they are closely related structures. The largest deviation is TS-1, which has a photoemission and vibrational modes that are higher in energy than all the other materials. This can be interpreted, consistent with postulated structures, as arising from a symmetry reduction in the titanium site imposed by the zeolite structure. It should be noted, however, that this is not definitive and all we can say is that TS-1 deviates markedly from tetrahedral and, therefore, the possibility of an alternate structure cannot be ruled out. Finally, it is also important to acknowledge that the emissive sites may not, in fact, be the catalytically active sites.

**Acknowledgment.** We are indebted to Claude Davis of Corning for helpful discussions and the donation of a test sample of ULE® glass. We also thank Dr. Vincent Salters, Ted Zateslo, and Afi Sachi-Kocher of the National High Magnetic Field Laboratory for performing ICP-MS on our samples and reagent. We also thank Dr. Walter Klemperer for helpful discussions.

## References and Notes

(1) McCulloch, S.; Stewart, G.; Guppy, R. M.; Norris, J. O. W. *Int. J. Optoelectron.* **1994**, *9*, 235−241.
(2) Evans, D. L. *J. Am. Ceram. Soc.* **1970**, *53*, 418−419.
(3) Davis, R. J.; Liu, Z. F. *Chem. Mater.* **1997**, *9*, 2311−2324.
(4) Notari, B. *Catal. Today* **1993**, *18*, 163−172.
(5) Notari, B.*Adv. Catal.* **1996**, *41*, 253−334.
(6) Soult, A. S.; Poore, D. D.; Mayo, E. I.; Stiegman, A. E. *J. Phys. Chem. B* **2001**, *105*, 2687−2693.
(7) Hayashi, T.; Yamada, T.; Saito, H. *J. Mater. Sci.* **1983**, *18*, 1983.
(8) Evans, J. S. O.; Mary, T. A.; Sleight, A. W. *Physica B* **1998**, *243*, 311−316.
(9) Vayssilov, G. N. *Catal. Rev.−Sci. Eng.* **1997**, *39*, 209−251.
(10) Ricchiardi, G.; Damin, A.; Bordiga, S.; Lamberti, C.; Spano, G.; Rivetti, F.; Zecchina, A. *J. Am. Chem. Soc.* **2001**, *123*, 11409−11419.
(11) Knight, D. S.; Pantano, C. G.; White, W. B. *Mater. Lett.* **1989**, *8*, 156−160.

(12) Pluth, J. J.; Smith, J. V.; Faber, J. *J. Appl. Phys.* **1985**, *57*, 1045−1049.
(13) Evans, D. L. *J. Non-Cryst. Solids* **1982**, *52*, 115−128.
(14) Schneider, H.; Majdic, A. *Neues Jahrb. Mineral.-Mon.hefte* **1985**, 418−426.
(15) Schneider, H.; Majdic, A. *Neues Jahrb. Mineral.-Mon.hefte* **1984**, 559−568.
(16) Dzwigaj, S.; Matsuoka, M.; Anpo, M.; Che, M. *J. Phys. Chem. B* **2000**, *104*, 6012−6020.
(17) Chiodini, N.; Meinardi, F.; Morazzoni, F.; Paleari, A.; Scotti, R.; Di Martino, D. *J. Non-Cryst. Solids* **2000**, *261*, 1−8.
(18) Rebohle, L.; von Borany, J.; Skorupa, W.; Frob, H.; Niedermeier, S. *Appl. Phys. Lett.* **2000**, *77*, 969−971.